



ELSEVIER

Available online at www.sciencedirect.com

SCIENCE @ DIRECT®

Nuclear Instruments and Methods in Physics Research A 515 (2003) 563–574

**NUCLEAR
INSTRUMENTS
& METHODS
IN PHYSICS
RESEARCH**

 Section A
www.elsevier.com/locate/nima

Progress toward a new measurement of the parity violating asymmetry in $\vec{n} + p \rightarrow d + \gamma$

W.M. Snow^a, W.S. Wilburn^b, J.D. Bowman^b, M.B. Leuschner^{c,*}, S.I. Penttilä^b,
V.R. Pomeroy^c, D.R. Rich^{a,1}, E.I. Sharapov^d, V.W. Yuan^b

^aDepartment of Physics, Indiana University, Bloomington, IN 47405, USA

^bLos Alamos National Laboratory, Los Alamos, NM 87545, USA

^cDepartment of Physics, University of New Hampshire, Durham, NH 38245, USA

^dJoint Institute for Nuclear Research, Dubna 141980, Russia

Received 11 June 2003; accepted 1 July 2003

Abstract

A proof-of-principle experiment using unpolarized low-energy neutron capture on polyethylene and an array of 12 CsI detectors operated in current mode has been performed to test the possibility of measuring at LANSCE the parity-violating asymmetry A_γ in the angular distribution of 2.23 MeV gamma rays from the $\vec{n} + p \rightarrow d + \gamma$ reaction. Results of this experiment including the current mode signal, electronic noise and detector sensitivity to magnetic fields are reported. The motivation and conceptual design for a new experiment aimed at a 10-fold improvement in the accuracy of A_γ are outlined.

© 2003 Elsevier B.V. All rights reserved.

PACS: 23.40.Bw; 24.80.+y

Keywords: Weak interaction and lepton aspects

1. Motivation

The weak interaction between nucleons can be described, in a theoretical meson-exchange framework, by a potential involving six weak meson–nucleon coupling constants. Those, in the notation

of Adelberger and Haxton [1], are: $H_\pi^1 = 1.1$, $H_\rho^0 = 1.6$, $H_\rho^1 = 0.03$, $H_\rho^2 = 1.3$, $H_\omega^0 = 0.8$, $H_\omega^1 = 0.5$, in units of 10^{-6} . In this notation, the subscript labels the meson involved and the superscript labels the change in isospin. Quoted values correspond to the DDH [2] recommended best values² of the weak coupling constants for the Weinberg–Salam model. However, the actual size of the weak coupling

*Corresponding author. Present address: Indiana University Cyclotron Facility, 2401 Milo B. Sampson Lane, Bloomington, IN 47408, USA. Tel.: +1-812-856-1721; fax: +1-812-855-6645.

E-mail address: leuschner@iucf.indiana.edu (M.B. Leuschner).

¹Present address: Department of Physics, Wabash College, Crawfordsville, IN 47933, USA.

²See e.g. Ref. [1] for the relationship between the values of coupling constants of Desplanques, Donoghue and Holstein (DDH) and the coupling constants of Adelberger and Haxton; in particular, $H_\pi^1 = F_\pi = f_\pi g_{\pi NN} / \sqrt{32}$, where $g_{\pi NN} = 13.45$ and f_π is the DDH weak coupling constant.

constants remains uncertain. The reasons for that are both experimental and theoretical. The experimental problems stem from the small size of weak amplitudes relative to strong amplitudes (typically $\approx 10^{-7}$ at low energies). The theoretical difficulties are encountered in trying to relate the underlying interactions between quarks to low-energy observables in the interaction between nucleons. The current approach is to split the problem into two parts. The first step is to map QCD to an effective theory expressed in terms of the most important low energy degrees of freedom—mesons and nucleons. In this process, the effects of quark–quark currents appear as the strong interaction couplings and the parity-violating weak meson–nucleon couplings [2]. The second step is to use this effective theory to calculate the parity violating effects in the nucleon–nucleon (NN) interactions and to determine the weak couplings from experiments.

The coupling constant for the π -meson exchange with the isospin change $\Delta I = 1$, H_π^1 , is of special interest because it is expected to be sensitive to weak neutral currents. It is also the longest range component of the weak NN interaction, and presumably its effects are well calculable in the NN system. The most reliable information on the strength of H_π^1 is believed to come from measurements of the circular polarization of 1081 keV gamma rays from ^{18}F [3,4]. The nuclear structure uncertainties complicate the analysis of the parity-violating effects in light nuclei. Nevertheless, the current ^{18}F results have been interpreted as an upper limit of the weak pion–nucleon–nucleon coupling, $H_\pi^1 \leq 0.34 \times 10^{-6}$. This value, which is 3σ smaller than the DDH best value of H_π^1 , has led to speculation that quark–quark neutral currents might be suppressed in $\Delta I = 1$ processes.

New information on H_π^1 comes from the recent observation of nuclear parity violation in an atomic parity-violation experiment in ^{133}Cs [5]. This experiment detected for the first time the parity-violating nuclear anapole moment. The interpretation of the experiment requires assumptions about nuclear structure. The value of H_π^1 inferred from this experiment in Refs. [6,7] is about twice the DDH best value and about factor of 6.5 larger than the upper limit set by the ^{18}F

experiments. At the same time, the DDH prediction for H_π^1 has sharpened to $0\text{--}0.6 \times 10^{-6}$ [8] due to improved knowledge of the QCD coupling constant and the treatment of quark masses. These developments have been discussed recently in Ref. [9] with the conclusion that accurate H_π^1 - and H_ρ^0 -measurements in the nucleon–nucleon system are needed to resolve these inconsistencies.

The NN systems are simple enough that the measured parity violation can be related to the weak couplings with negligible uncertainty due to nuclear structure. In particular, parity-nonconserving (PNC) effect in the reaction $\bar{n} + p \rightarrow d + \gamma$ is almost entirely due to weak pion exchange. The PNC asymmetry A_γ , in other words, the correlation between the direction of emission of the gamma ray and the neutron polarization, is calculated to be [10–12]

$$A_\gamma = -0.045(H_\pi^1 - 0.02H_\rho^1 + 0.02H_\omega^1 + 0.04H_\rho^1). \quad (1)$$

For the DDH best values of the weak coupling constants one concludes that the ρ - and ω -meson couplings contribute only at the few-percent level. Unfortunately, existing measurements of A_γ [13,14] have insufficient precision: the latest result is $A_\gamma = -1.5 \pm 4.8 \times 10^{-8}$ [14]. This value is neither sensitive enough to address the inconsistencies in the size of H_π^1 , nor to reach the range of values for H_π^1 predicted by theories [2,15–17].

In this paper, we discuss a proof-of-principle for a new experiment to measure A_γ with a precision of $\pm 0.5 \times 10^{-8}$ which will determine H_π^1 to $\pm 0.1 \times 10^{-6}$ (see Fig. 1). Such a result will clearly

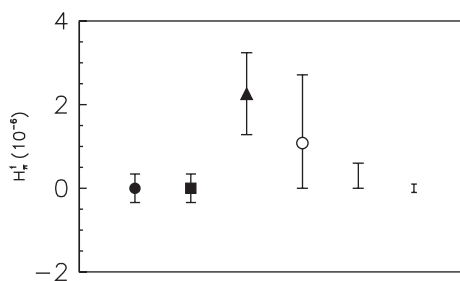


Fig. 1. Values of H_π^1 from (left to right): the earlier npdy experiment, ^{18}F experiments, ^{133}Cs experiment, DDH theoretical estimate, the latest theoretical estimate, the proposed experiment. References and explanation are found in the text.

distinguish between the ^{18}F and ^{133}Cs values for H_{π}^1 as well as between different predictions given by theories of the weak interaction of hadrons in the non-perturbative QCD regime. There is also a strong possibility that a non-zero result for A_{γ} will be seen which will fix the value of H_{π}^1 .

2. Requirements for an accurate measurement of A_{γ} in the reaction $\bar{n} + p \rightarrow d + \gamma$

To determine H_{π}^1 with an uncertainty of 0.1×10^{-6} , 10% of the DDH best value, we need a statistical uncertainty of 0.5×10^{-8} on A_{γ} which means that we have to detect about 4×10^{16} gammas from the $\bar{n} + p \rightarrow d + \gamma$ reaction. In addition, we have to keep the systematic errors below the statistical error. Among the essential aspects of the proposed experiment which led us to the choice of issues to be addressed in the proof-of-principle experiment, are the following:

- (1) The number of events required to achieve sufficient statistical accuracy in a reasonable time immediately leads to the conclusion that the 2.23 MeV gamma rays must be counted in current mode.
- (2) Neutron fluxes available at present neutron sources are not high enough to achieve the required statistical accuracy in a small amount of time. Therefore, it is important to demonstrate that the electronic noise introduced by the current-mode measurement technique is negligible compared to the shot noise due to the discrete nature of the charge deposited by each gamma ray and number of photoelectrons produced.
- (3) The tiny parity violating signal will be isolated by flipping the neutron spin, since the real asymmetry will change sign under spin reversal, while spin-independent false asymmetries will not. The neutron spin can be flipped by either static or RF magnetic fields. It is essential to measure the sensitivity of the detector efficiency to magnetic fields and show that the systematic effect introduced by the magnetic fields to the asymmetry is much smaller than the statistical error.

There are a host of other issues to be addressed, including spurious systematic effects, production and delivery of the polarized neutrons to the protons, details of the neutron spin flipping, etc. However, the three issues mentioned above would render the experiment impossible if unresolved. Therefore, we constructed an experiment to address these questions.

3. Experiment

A proof-of-principle experiment was performed by the time-of-flight (TOF) method at the pulsed spallation source of the Los Alamos Neutron Science Center (LANSCE) where neutrons are produced by impinging 800 MeV proton pulses at a repetition rate of 20 Hz from the Proton Storage Ring to the tungsten spallation target surrounded by a water moderator [18]. The neutron flux spectrum from the Gd-poisoned room temperature water moderator has a Maxwellian thermal-energy component and an epithermal tail which falls off approximately as $1/E$. Owing to the TOF specifics, the instantaneous intensity of the neutron beam is higher in the epithermal region than in the Maxwellian. We chose an incident neutron energy of about 1 eV, so that the detected rates of 2.23 MeV gammas from neutron capture on hydrogen would correspond to the rates expected for the cold neutron moderator in the future parity-violating experiment.

With the proton current of 70 μA the epithermal neutron spectral intensity on the target, the number of neutrons ΔN with energies between E and $E + \Delta E$ per proton pulse, is calculated to be [19]

$$\Delta N = \frac{1.0 \times 10^{11}}{E^{0.95}} f \Omega \Delta E \frac{\text{neutrons}}{\text{pulse}}. \quad (2)$$

Here f is the fraction of the 13 cm \times 13 cm moderator viewed by the target through the collimators, and Ω is the solid angle in steradians ($\Omega = S/L^2$, where S is the target area exposed to the neutron beam and L is the length of the flight path). The experiment was mounted on the neutron flight path #2 at $L = 6.4$ m from the source after a 10-cm diameter collimation system.

The target was a 15 cm diameter by 5 cm thick disk of polyethylene supported by a 2 cm thick cylindrical polyethylene shell inserted into the detector annulus. The incident neutrons were thermalized in a polyethylene target and the 2.23-MeV gamma rays from the neutron capture in hydrogen were detected by a CsI detector assembly [20]. For calibration measurements a second target, an indium foil, was also used. CsI(pure) crystals were arranged around the target in an annulus having an inner diameter of 20 cm, an outer diameter of 40 cm, and a length of 13 cm, so that the detector was subtended a solid angle of 3.0 sr relative to the target. This arrangement is shown schematically in Fig. 2. The detector system was shielded by a 10 cm thick lead housing with holes for the beam entry and exit.

The scintillation light from the CsI crystals was measured directly by individual phototubes (Hamamatsu R5004). Current signals were taken from the photocathodes. All other phototube elements, including dynodes, were connected to a battery and biased to +90 V with respect to the cathodes. Two different electronic configurations were tested. In the first, only two individual photocathodes were connected to low-noise preamplifiers attached directly to the phototube sockets. The amplified signals were then connected to an NIM module which formed sum and difference signals. This arrangement was used to measure the electronic noise and is similar to

design for the proposed measurement, where each photocathode will have an individual preamplifier. In the second configuration all 12 CsI detectors were used, the photocathodes were connected together in two groups of six, top and bottom. The two signals from each group were amplified and then connected to the summing and differential amplifiers, as described above. This circuit was used to study fluctuations in the capture gamma ray yield, due to effects such as beam intensity and position modulations. With this circuit, we could measure the spectral density of the beam noise.

Fig. 3 shows the yield of the gamma ray detector with the indium target in place as a function of a neutron time-of-flight (t.o.f. for 1 eV neutrons is about 463 μ s at 6.4 m): the peaks at t.o.f. 152, 235, and 380 μ s are the indium neutron resonances at 9.07, 3.85, and 1.46 eV, respectively. The signals were taken from the photocathodes of the photomultiplier tubes and then amplified by preamplifiers. The first goal of the test experiment was to verify that in the current-mode operation the electronic noise of the detector system can be reduced below the shot noise; the statistical fluctuations of the current due to the finiteness of the deposited energy of the gammas or the number of photoelectrons produced per event. The second goal of the test experiment was to measure the sensitivity of the detector efficiencies to magnetic fields.

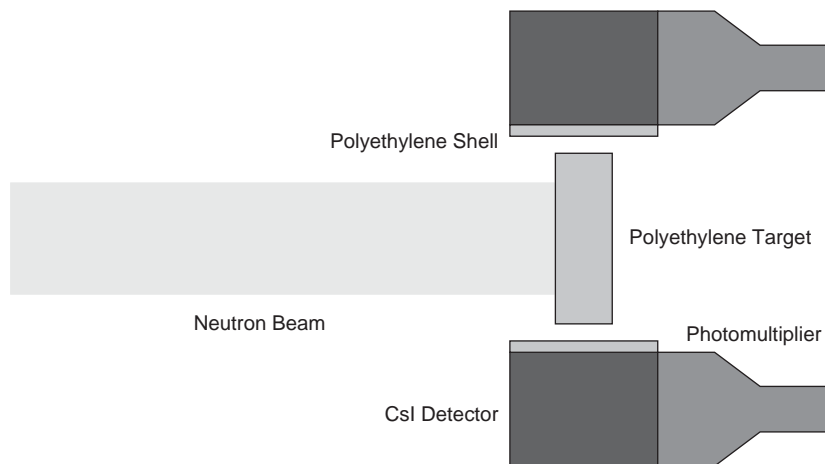


Fig. 2. Experimental arrangement for the test experiment, showing the neutron beam, polyethylene target, and CsI detectors.

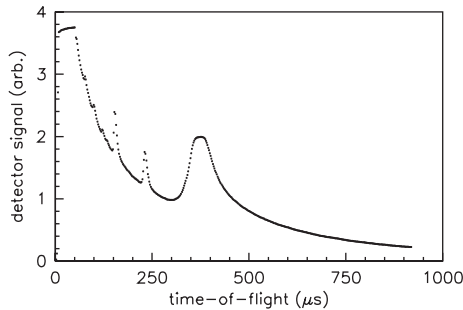


Fig. 3. The yield of the gamma ray detector with the indium target as a function of neutron time-of-flight. The three distinct peaks are neutron resonances in indium.

3.1. Current mode signal

Several measurements were performed to ensure that the observed detector current for the full array, $(0.56 \pm 0.01) \mu\text{A}$ for 1 eV neutrons, was consistent with calculations based on the yield of neutron capture gamma rays from hydrogen in the polyethylene target. This number is the product of the neutron flux, probability for the neutron to capture on a proton, probability that the capture produces a gamma ray which absorbs in the detector, and the charge per gamma ray which appears at the photocathode. The instantaneous value of $(5.0 \pm 0.7) \times 10^{10} \text{ s}^{-1}$ for flux of 1 eV neutrons on the target was calculated from Eq. (2) by the use of identity $\Delta E/E = 2\Delta t/t$. The uncertainty in the flux was inferred from the absolute flux measurement of Ref. [21] performed at the same beam of the flight path #2. The neutron flux given by Eq. (2) agrees with this measurement.

A Monte-Carlo calculation was performed to estimate the fraction (approximately 60%) of incident neutrons which capture on protons in the polyethylene target after moderation. Most of the remaining neutrons backscatter from the target. The mean free path of 5 mm for thermal neutrons in polyethylene was used in the calculations and was verified by relative transmission measurements. The prediction for the amount of backscattered neutrons was tested by moving the location of the target relative to the detector array and observing that the target position which gave the largest detector signal was located about 6 cm downstream from the center of the detector

annulus. The large size of the signal at this position, about 2.5 times larger than the signal for the target centered on the array, was attributed to backscattered neutrons which capture on the protons in the cylindrical polyethylene support structure for the target (gamma rays from the support are closer to the detectors and have a larger solid angle).

Since the solid angle was known, the only remaining quantity needed to calculate for the detector current was the number of photoelectrons produced in the photocathodes of the CsI detectors by the 2.23 MeV gamma ray. This number was determined by two independent methods. First, the polyethylene target was replaced by a 0.3 mm thick In foil. At 1.46 eV indium possesses a strong neutron resonance which captures all the neutrons from the beam. The resonance state decays primarily via gamma emission. Using the measured detector current at the resonance, we inferred a value of 70 photoelectrons/MeV of deposited gamma ray energy. This number was consistent within errors with the value of 65 photoelectrons/MeV inferred from the energy resolution measurement of the CsI detectors with a ^{60}Co gamma source. The number of photoelectrons per MeV was calculated under the assumption that the energy resolution is dominated by the statistical fluctuations of the number of photoelectrons.

Based on this combination of measurements and simulations, the predicted detector current for the full array of 12 detectors is $0.5 \pm 0.1 \mu\text{A}$ for 1 eV neutron rate. The agreement with the measured value of $(0.56 \pm 0.01) \mu\text{A}$ has two consequences: (1) the current-mode signal is indeed dominated by gamma rays from neutron capture on protons, (2) the value for the number of photoelectrons per MeV in the detector is determined. This value is needed to calculate the expected amount of noise in the detector array due to current shot noise from neutron counting statistics.

3.2. Electronic noise

The detector electronics used for the noise measurements are shown in Fig. 4. The circuit consists of two low-noise current-to-voltage (IV)

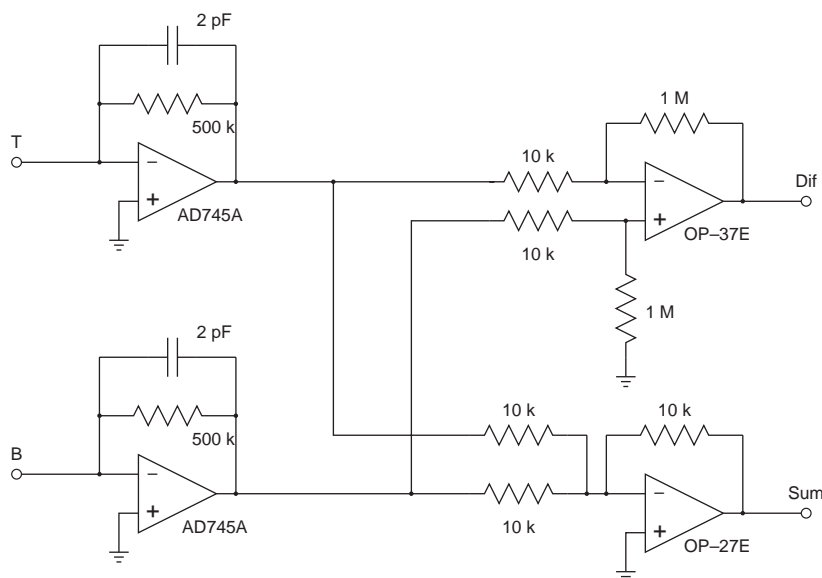


Fig. 4. Diagram of the detector front-end electronics for the test experiment.

amplifiers, followed by stages which take the sum and difference of the two voltages. The IV amplifiers were designed using AD745A op-amps. These op-amps have a typical voltage noise density of $2.9 \text{ nV}/\sqrt{\text{Hz}}$ and typical current noise density of $6.9 \text{ fA}/\sqrt{\text{Hz}}$ at 1 kHz. The $500 \text{ k}\Omega$ feedback resistor gives a DC gain of $0.5 \text{ V}/\mu\text{A}$ and contributes a noise density of $180 \text{ fA}/\sqrt{\text{Hz}}$. A 2 pF feedback capacitor limits the noise bandwidth to 250 kHz. Precision resistors (0.1%) with low temperature coefficients ($20 \text{ ppm}/^\circ\text{C}$) are used in the IV, summing, and differential amplifier stages. The summing circuit was designed to have an overall gain of $0.5 \text{ V}/\mu\text{A}$, and the differential circuit a gain of $50 \text{ V}/\mu\text{A}$. The spectral density measurement used the same circuit with the preamplifier gain reduced by a factor of 50 and the bandwidth of 160 kHz.

Using a digital oscilloscope (LeCroy model TDS 744A) the electronic noise of the detector was determined for the sum and difference outputs. The noise of the sum output was $760 \mu\text{V}_{\text{rms}}$. This corresponds to $2.2 \text{ pA}/\sqrt{\text{Hz}}$ at each input. The difference output had $11 \mu\text{V}_{\text{rms}}$ noise, corresponding to $0.3 \text{ pA}/\sqrt{\text{Hz}}$ at each input. It is useful to compare the difference noise to the rms shot noise

created by the quantized nature of the expected detector signal

$$I_{\text{sn}}/\sqrt{f} = \sqrt{2qI} \quad (3)$$

where q is the charge generated in the photocathode per gamma and I is the photocathode current. Using the expected values $q \approx 150e$ and $I \approx 100 \text{ nA}$, we obtain $I_{\text{sn}}/\sqrt{f} \approx 2 \text{ pA}/\sqrt{\text{Hz}}$, a factor of 7 greater than our electronic noise. Theoretically, an electronic noise of just $0.2 \text{ pA}/\sqrt{\text{Hz}}$ should be obtainable. We attribute the excess noise observed in our test to electromagnetic pickup. This contribution will be reduced with improved electrostatic shielding.

3.3. Spectral density

Periodic variations in experimental parameters can produce false asymmetries. These effects include fluctuations in detector gain, beam intensity and beam position, which are expected to dominate over other fluctuations. The proposed experiment has been designed so that these fluctuations do not contribute to a false asymmetry in first order. Since the parity-violating asymmetry is formed by taking the difference

between up and down detector currents, the two currents are measured simultaneously, making the apparatus quite insensitive to incident flux variations. Second, the azimuthal symmetry of the apparatus suppresses the contribution from the beam motion. While such effects do not lead directly to false asymmetries, it is possible for them to contribute in higher order. For example, the beam motion combined with detector-efficiency differences can give a non-zero effect. For this reason, it is important to know the size of the beam fluctuations.

We measured the influence of these fluctuations on the detector signal and set an upper limit for their contribution. We sampled the difference signal from the detectors every 50 ms (every beam pulse) by integrating the voltage in a 1 μ s window at constant t.o.f. during a 20 min period while the spallation source operated in a steady-state mode. The autocorrelation function of the difference signal, $f(\tau) = \langle i(t)i(t-\tau) \rangle$ was then calculated. The Fourier transform of this quantity, $F(\omega) = \int_{-\infty}^{+\infty} f(\tau)e^{i\omega\tau} d\tau$, is the spectral density of the intensity fluctuations of the neutron source as filtered through the difference signal. There were no periodic sources of noise observed in the 0–10 Hz range (Fig. 5). The upper limit of this range is set by the sampling rate, which is in turn limited by the pulse spacing. Because the circuit bandwidth (160 kHz) was larger than this upper observable frequency, the noise above 10 Hz is aliased into the 0–10 Hz range. Correcting for this effect, we estimate an upper limit of 5 fA/ $\sqrt{\text{Hz}}$ on beam-induced fluctuations on the difference signal.

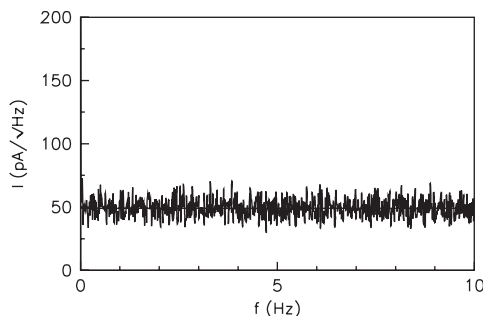


Fig. 5. Spectral density of the detector difference signal due to the neutron beam fluctuations.

3.4. Detector sensitivity to magnetic fields

The primary techniques for reducing the false asymmetries generated by the experimental fluctuations is the fast reversal of the neutron spin. Depending on the reversal techniques it will introduce changing magnetic fields which can effect the efficiency of the detector. Therefore, it was important to measure the sensitivity of the detector to magnetic fields. The measurement was performed by applying a 10 G magnetic field to the detectors using a pair of 76 cm diameter coils. The field direction was reversed every 10 s. The field was oriented parallel to the photocathode surfaces of the photomultiplier tubes in an attempt to maximize the size of the effect. The observed change in the detector efficiency was $2 \times 10^{-5} \text{ G}^{-1}$. This is about five orders of magnitude smaller than one would expect for a typical photomultiplier tube operated in the normal fashion with high voltage on the dynodes and the signal measured from the anode.

Changes in static magnetic fields at the detectors upon a spin flip must therefore be held below the 10 μ G level. Spin flipping by RF magnetic fields would be preferable, since one expects the detectors and associated electronics to be even less sensitive to such fields. In particular we envisage the use of a spin flipper working at 30 kHz RF field with an amplitude of 0.3–3 G placed in aluminum shield.

The conclusions of the test measurements are that the noise introduced by the current-mode detection is less than the shot noise and the magnetic field sensitivity of the detector is very low when the signals are taken from the photocathodes.

In the remainder of the paper, we discuss a conceptual design of the experiment based on the results of the test experiment, an estimate for the statistical accuracy, and diagnostics for some classes of systematic effects.

4. Conceptual design of $\bar{n} + p \rightarrow d + \gamma$ experiment

We briefly describe in this section a conceptual design of the future experiment, and we discuss

those aspects which are particularly important for its implementation. Fig. 6 shows the elements of the design.

The $\bar{n} + p \rightarrow d + \gamma$ experiment requires a high flux of cold neutrons with energies below 15 meV, as will be explained later. While such neutrons are available from cold moderators at both reactors and spallation neutron sources, the pulsed nature of the neutron flux from a spallation source provides a diagnostic tool for a number of systematic effects for this experiment. At LANSCE the cold neutron source is a liquid hydrogen moderator coupled to the 20 Hz pulsed neutron source. The neutron spectrum consists of a Maxwellian component with a maximum at about 4 meV and width set by the effective temperature of the moderator (approximately 50 K) and an epithermal component with an approximately $1/E$ spectrum (Fig. 7). With the use of a neutron guide the neutron spectrum at the target will be enhanced at low energies because the guide reflects neutrons with transverse momentum components below a characteristic critical value and therefore transmits (from the moderator to the target) a larger fraction of the phase space for lower momentum neutrons.

The experiment requires polarized neutrons. We plan to use a polarized ^3He neutron-spin filter (see Ref. [22] and references therein). Polarized ^3He gas acts as a transmission polarizer. The total cross-section for the ^3He nucleus is very large for the $J = 0$ capture channel and about four orders of

magnitude smaller for the $J = 1$ channel. The neutron polarization (P) and transmission (T) properties are therefore strongly dependent on ^3He polarization: an example is shown in Fig. 8. An expected ^3He polarization for the future experiment is about 60%.

The parity-violating signal will be isolated by periodically reversing the neutron spin. The spin flipper must be capable of rapidly and reproducibly reversing the beam polarization in a broad range of cold neutron energies with essentially unit efficiency over the entire beam profile with no effect on the gamma detectors. The fast (20 Hz) spin reversal is possible with a spin flipper which uses RF magnetic fields [23]. The reversal of the neutron polarization then consists of turning the RF magnetic field on and off, which can be carried

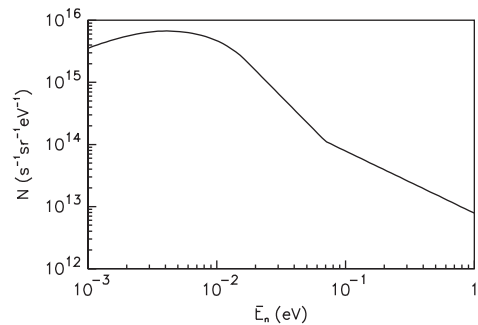


Fig. 7. The calculated neutron spectrum for the LANSCE coupled LH_2 moderator. This is the total neutron flux from the $13\text{ cm} \times 13\text{ cm}$ moderator surface with the average proton current of $200\ \mu\text{A}$.

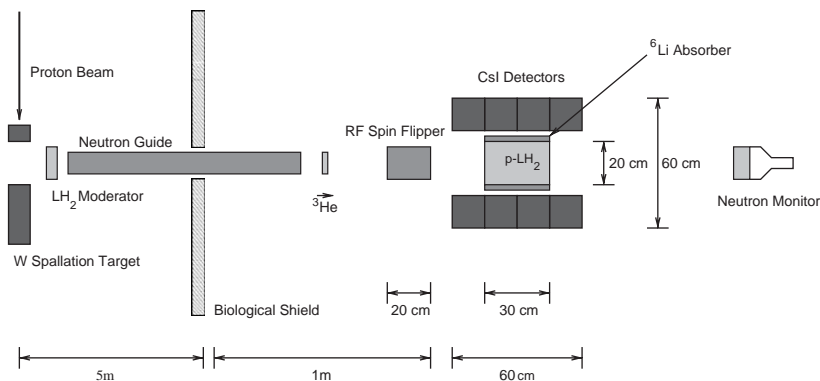


Fig. 6. The conceptual design for the $\bar{n} + p \rightarrow d + \gamma$ experiment, showing the most important elements (not to scale). Approximate sizes and distances are indicated for some features.

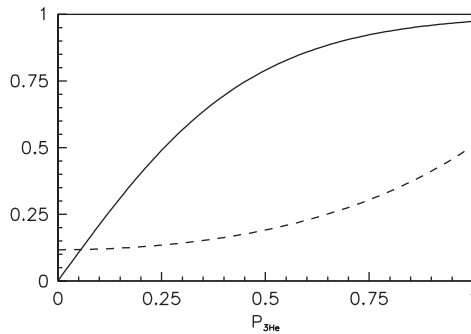


Fig. 8. Polarization (solid) and transmission (dash) of 4 MeV neutrons after passage through a 6 atm cm ^3He cell, as a function of ^3He polarization.

out quickly enough to flip the neutron polarization on every beam burst at 20 Hz. The gamma detectors can be efficiently shielded from the RF magnetic field with a thin metal enclosure. Neutron spin flippers based on the reversal of an otherwise static magnetic field suffer primarily from the greater difficulties of shielding static magnetic fields and the relatively higher sensitivity of the gamma detector efficiency to static fields.

In order for the experiment to be clearly interpretable as a measurement of parity violation in the neutron–proton system, a target of pure hydrogen is required. Clearly, it is essential that the polarized neutrons retain their polarization until they capture. It is therefore important to consider the spin dependence of the scattering. The ground state, the para state, of the hydrogen molecule has $J = L = S = 0$, and the first excited state, the lowest ortho state, is 15 meV above the para state. A large fraction of the cold neutrons possess energies lower than 15 meV. Since these neutrons cannot excite the para-hydrogen molecule, only elastic scattering and capture are allowed, and spin-flip scattering is forbidden. The neutron polarization therefore survives the large number of scattering events which occur before the capture. Higher energy neutrons will undergo spin-flip scattering and will therefore depolarize. This is the reason for the requirement of neutrons with energies below 15 meV.

We must prepare a 21-l liquid hydrogen target in the para state. For liquid hydrogen held at 20 K and atmospheric pressure the equilibrium concen-

tration of para-hydrogen is 99.8%, low enough to ensure a negligible population of ortho-hydrogen. Such a target will convert approximately 60% of the incident neutrons to gamma rays according to the MCNP calculations.

Finally, we discuss requirements for detecting gamma rays from the hydrogen target to measure the very small asymmetry $A_\gamma \simeq 0.5 \times 10^{-8}$. Of course, current-mode gamma detection is required. The gamma detector must have a high efficiency which is unaffected by neutron spin reversal and radiation damage. The detector should cover a large solid angle, and segmentation of the detector is required to resolve the angular dependence of the expected parity-violating signal and discriminate false effects. For example, there is a predicted parity-conserving gamma asymmetry of $A_\gamma^{\text{PC}} = 0.8 \times 10^{-8}$ [24] in the np capture. This process gives an asymmetry about the same magnitude as our sensitivity goal for the parity violating signal, but with an angular distribution orthogonal to the parity violating signal. The segmentation of the detector allows separation of the parity-violating and parity-conserving asymmetries.

Alkali iodine crystals are well suited for the gamma ray detection because of their high density, 4.5 g/cm³. Three interaction lengths (3×5.5 cm) thick crystal will stop 95% of the 2.2 MeV gamma rays. Our plan is to use cubes of CsI(Tl) crystals approximately 15 cm on a side coupled to the Hamamatsu R2046PT photo diodes operated in current mode. The signal is taken directly from the photocathode to decrease the sensitivity of detector gain to magnetic fields, as in the test experiment. Based on previous studies, these detectors should be capable of withstanding the integrated gamma dose in the experiment without serious effects on the detector efficiency [25]. They were used successfully in our test runs to perform current-mode counting at the expected instantaneous rates of $\sim 10^{11}$ gammas per second.

The gamma detectors must be shielded from neutrons scattered from the hydrogen target. The isotope ^6Li is the ideal material for this purpose due to its large neutron absorption cross-section, most of which proceeds by a breakup channel to a triton and alpha in their ground states, thus producing no gamma rays.

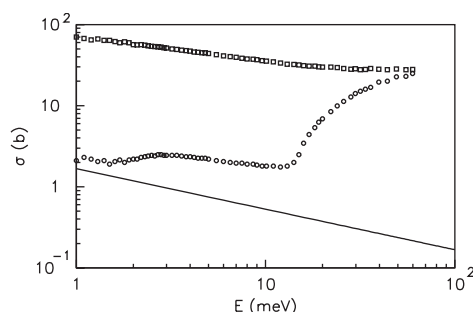


Fig. 9. Measured scattering cross-sections for neutrons on para-hydrogen (circles) and neutrons on normal hydrogen (squares). The solid line is the cross-section for np capture.

In addition to its primary purpose of monitoring the beam intensity, the beam monitor can be used to detect changes in the concentrations of ortho-hydrogen and para-hydrogen in the target. This is possible due to the very large difference in neutron cross-sections for the two species at low neutron energies (see Fig. 9) [26]. At 4 meV neutron energy, for example, the ortho-hydrogen cross-section is 20 times larger than the para-hydrogen cross-section. Even small changes in the equilibrium ortho-hydrogen concentration in the target will therefore lead to large changes in the transmitted neutron flux.

Next we estimate briefly the statistical accuracy of the experiment at the LANSCE spallation neutron source. The estimate has been done under the following assumptions:

- (1) The time-averaged brightness from a coupled liquid hydrogen moderator is given by Fig. 7.
- (2) A 15 m long, 10 cm \times 10 cm cross section supermirror neutron guide is mounted 1 m from the moderator. The transmission of the guide is assumed to be 100% for neutrons with angles of incidence less than the critical angle which is assumed to be 3 times that for ^{58}Ni .
- (3) A 60% polarized ^3He neutron filter of a 4.5 atm cm thickness.
- (4) A 30 cm long, 30 cm diameter cylindrical liquid para-hydrogen target is mounted on the neutron beam.
- (5) The segmented 4π CsI(Tl) detector array is used to determine which hemisphere the gamma ray enters.

- (6) The uncertainty in the gamma flux striking detector, operated in current mode, is dominated by gamma ray counting statistics.

Under these assumptions and for 1 year of counting, a Monte-Carlo simulation gave a statistical error of 0.6×10^{-8} in A_γ . This statistical accuracy suffices to reach the goal of the experiment.

5. About systematic uncertainties

The most challenging aspect of the experiment is to design an apparatus which is: (a) insensitive to spurious systematic effects, (b) incorporates a large number of independent methods to isolate a true parity-violating signal, and (c) is flexible enough to allow the size of as many systematic effects as possible to be magnified artificially. The most dangerous class of systematic effects are those correlated with the neutron spin reversal, either through the direct physical effects due to the interaction of the neutron spin itself or through indirect effects on the gamma ray detection efficiency correlated with the neutron spin flipping process.

A detailed analysis of systematic effects lies outside the scope of this paper, and we refer the interested reader to another presentation [27]. However, we can point to aspects of the design of the experiment which are important for the study and isolation of systematic effects.

At a pulsed neutron source, the arrival time of the neutrons at the experiment after the proton pulse strikes the spallation target depends on the neutron energy: $t \propto 1/\sqrt{E}$. The relation between the neutron energy and the timing of the gamma ray signal is blurred somewhat by the distribution of moderation times of the neutrons first in the LH₂ moderator of the spallation source and then in the hydrogen target (which averages about 100 μs), but this effect is small in comparison to the flight times of the neutrons of interest (for instance, a 4 meV neutron needs 18 ms for a 16 m flight). Therefore, the time dependence of the gamma ray signal can be correlated with the incoming neutron energies.

The time-of-flight information is very useful for isolating and identifying systematic effects simply because different effects possess different dependences on neutron energy. For example, a systematic effect associated with the neutron beam motion due to the Stern–Gerlach effect in a gradient magnetic field in the spin transport system grows as the square of the time spent in the field gradient, and thus increases as a function of time-of-flight. On the other hand, a systematic effect from parity-conserving left-right scattering asymmetries coupled to detector asymmetries grows with the incident neutron energy and therefore decreases with time-of-flight. Each systematic effect has a characteristic time signature which can be used as a partial means of identification. Most of these time signatures are different from that expected from the true signal.

As noted in Section 4, neutrons with energies above 15 meV tend to depolarize before they capture. This not only effectively turns off the parity violating signal, but also all systematic effects which require the neutrons to be polarized in the para-hydrogen target. For example, effects induced by left-right scattering asymmetries in para-hydrogen must vanish above 15 meV. On the other hand, systematic effects not associated with polarized neutrons on hydrogen, such as bremsstrahlung from the parity-violating beta decay of window materials of the LH₂ target cryostat, will still be present at neutron energies above 15 meV.

6. Conclusions and summary

A sensitive measurement of the parity-violating gamma asymmetry in the reaction $\vec{n} + p \rightarrow d + \gamma$ can give definitive information on one of the most important and interesting components of the weak NN interaction. We have successfully tested a current-mode detector concept for the gamma rays and verified that its precision is limited only by gamma ray counting statistics. We have demonstrated that the efficiency of our current-mode gamma detector is insensitive to changes in magnetic field, the most important external parameter used to change the sign of the parity-violating signal in the experiment. The realization

of all other aspects of the experimental design appears to pose no insuperable technical difficulties. We have discussed a realistic experimental design which has the potential to be free of systematic effects at the required level and incorporates a number of powerful diagnostics to isolate systematic effects.

We conclude that an experiment is now feasible to search for the parity-violating gamma asymmetry A_γ in the reaction $\vec{n} + p \rightarrow d + \gamma$ with a sensitivity which is likely to obtain a non-zero result for A_γ and, consequently, for the weak coupling constant H_π^1 . A knowledge of H_π^1 will stimulate further development of the theory of the parity-violating effects based on the standard model description of the weak interaction and a QCD description of strong interactions.

Acknowledgements

This work has benefited from the use of the Los Alamos Neutron Science Center at the Los Alamos National Laboratory. This facility is funded by the U.S. Department of Energy and operated by the University of California under Contract W-7405-ENG-36.

References

- [1] E.G. Adelberger, W.C. Haxton, *Ann. Rev. Nucl. Part. Sci.* 35 (1985) 501.
- [2] B. Desplanques, J.F. Donoghue, B.R. Holstein, *Ann. Phys.* 124 (1980) 449.
- [3] H.C. Evans, G.T. Ewan, S.-P. Kwan, et al., *Phys. Rev. Lett.* 55 (1985) 791; S.A. Page, H.C. Evans, G.T. Ewan, et al., *Phys. Rev. C* 35 (1987) 1119.
- [4] M. Bini, T.F. Fazzini, G. Poggi, N. Taccetti, *Phys. Rev. Lett.* 55 (1985) 795.
- [5] C.S. Wood, S.C. Bennett, D. Cho, B.P. Masterson, J.L. Roberts, C.E. Tanner, C.E. Wieman, *Science* 275 (1997) 1759.
- [6] V.V. Flambaum, D.W. Murray, *Phys. Rev. C* 56 (1997) 1641.
- [7] W.C. Haxton, C.-P. Liu, M.J. Ramsey-Musolf, *Phys. Rev. Lett.* 86 (2001) 5247.
- [8] B. Desplanques, in: N. Auerbach, J.D. Bowman (Eds.), *Parity and Time Reversal Violation in Compound Nuclear*

- States and Related Topics, World Scientific, Singapore, 1996, p. 98.
- [9] W.S. Wilburn, J.D. Bowman, *Phys. Rev. C* 57 (1998) 3425.
- [10] B. Desplanques, *Nucl. Phys. A* 242 (1975) 423;
B. Desplanques, *Phys. Lett. B* 512 (2001) 305.
- [11] B.H.J. McKellar, *Nucl. Phys. A* 254 (1975) 349.
- [12] D.B. Kaplan, M.J. Savage, R.P. Springer, M.B. Wise, *Phys. Lett. B* 449 (1999) 1;
M.J. Savage, *Nucl. Phys. A* 695 (2001) 365.
- [13] J.F. Cavaignac, B. Vignon, R. Wilson, *Phys. Lett. B* 67 (1977) 148.
- [14] J. Alberi, R. Hart, E. Jeenick, et al., *Can. J. Phys.* 66 (1988) 542.
- [15] D.B. Kaplan, M.J. Savage, *Nucl. Phys. A* 556 (1993) 653.
- [16] E.M. Henley, W.-Y. Hwang, L.S. Kisslinger, *Phys. Lett. B* 367 (1996) 21 (errata: *Phys. Lett. B* 440 (1998) 449).
- [17] U.G. Meissner, H. Weigel, *Phys. Lett. B* 447 (1999) 1.
- [18] P.W. Lisowski, C.D. Bowman, G.J. Russell, S.A. Wender, *Nucl. Sci. Eng.* 106 (1990) 208.
- [19] P.D. Ferguson, G.J. Russell, E.J. Pitcher, in: ICANS-XIII: Proceedings of the Thirteenth Meeting of the International Collaboration on Advanced Neutron Sources, Paul Scherrer Institut Report PSI-Proceedings 95-02, Villigen, Switzerland, 1995, p. 510.
- [20] S.J. Seestrom, C.M. Frankle, J.D. Bowman, et al., *Nucl. Instr. and Meth. A* 433 (1999) 603.
- [21] N.R. Roberson, C.D. Bowman, J.D. Bowman, et al., *Nucl. Instr. and Meth. A* 326 (1993) 549.
- [22] D.R. Rich, J.D. Bowman, B.E. Crawford, et al., *Nucl. Instr. and Meth. A* 481 (2002) 431.
- [23] S.V. Grigoriev, A.I. Okorokov, V.V. Runov, *Nucl. Instr. and Meth. A* 384 (1997) 451.
- [24] A. Csótó, B.F. Gibson, G.L. Payne, *Phys. Rev. C* 56 (1997) 631.
- [25] Zong-ying Wei, Ren-yuan Zhu, *Nucl. Instr. and Meth. A* 326 (1993) 508.
- [26] W.D. Seiffert, B. Weckermann, R. Misenta, *Z. Naturforsch* 25a (1970) 967;
W.D. Seiffert, Technical Report No. EUR 4455d, 1970, Euratom.
- [27] W.M. Snow, C.S. Blessinger, G. Hansen, et al., in: C.R. Gould, G.L. Greene, F. Plasil, W.M. Snow (Eds.), *Fundamental Physics with Pulsed Neutron Beams*, World Scientific, Singapore, 2001, p. 203.